INFLUENCE OF LOW-TEMPERATURE ANNEALING BEFORE FIRING ON LETID IN MULTICRYSTALLINE SILICON

Andreas Schmid, Jeanette Lindroos, Annika Zuschlag, Daniel Skorka, Jakob Fritz, Giso Hahn
University of Konstanz, Department of Physics, 78457 Konstanz, Germany

ABSTRACT: Light and elevated temperature induced degradation (LeTID) affects significantly the performance of multicrystalline silicon (mc-Si) solar cells. The underlying mechanisms of LeTID and following regeneration are still unknown. Based on minority charge carrier lifetime (τ_{eff}), the influence of sample thickness, as well as the impact of low temperature annealing *before* firing and therefore introduction of hydrogen on material quality of mc-Si samples was tested. Afterwards the degradation and regeneration behavior under illumination (1.0 ±0.1 suns) and elevated temperature (150°C) was investigated. The samples were measured repetitively using photoconductance decay (PCD) at elevated temperature (150°C) and by time-resolved photoluminescence imaging at room temperature at selected points in time. The spatially resolved maps of τ_{eff} are analyzed, and with the extracted PCD data at fixed charge carrier density of $\Delta n = 1.5 \times 10^{15}\ \text{cm}^{-3}$ the normalized defect density was calculated. This approach leads to detailed analysis of the investigated mc-Si samples and might help to better understand the underlying LeTID defect. It could be shown that thinner samples show lower initial τ_{eff} and less LeTID. Furthermore, a pre-annealing step before firing impacts τ_{eff} and the firing step does not erase the thermal history. Finally, samples treated in H-atmosphere showed a detrimental effect of hydrogen in areas with high τ_{eff} and stronger LeTID compared to samples treated in nitrogen atmosphere.

Keywords: Degradation, Multicrystalline Silicon, Annealing, Lifetime, Hydrogen, LeTID

1 INTRODUCTION

Multicrystalline (mc) Si PERC (passivated emitter and rear cell) solar cells, but also lifetime samples, show a strong degradation under illumination at elevated temperatures (*e.g.* [1-4]), so-called light and elevated temperature induced degradation (LeTID). The already known degradation mechanisms like dissociation of FeB pairs and BO-correlated defects cannot explain the observed degradation kinetics [1-3]. Solar cells [3] as well as lifetime samples [5] also show a regeneration process after degradation. The underlying mechanisms causing the degradation and regeneration of mc-Si are still unknown. However, it could be shown that material properties like sample thickness [6] and treatment conditions like illumination and temperature (*e.g.* [3, 7]) influence the kinetics of degradation and regeneration. Furthermore, a low temperature dark annealing step *after* firing is known to impact LeTID formation in mc-Si [8]. However, as LeTID only forms at firing temperatures above 675°C [9], the firing step is presumed to dominate over any preceding low temperature steps. Interestingly, the surface passivation layer has been shown to also influence the LeTID defect density [10]. Passivation layers were deposited with different PECVD (plasma-enhanced chemical vapor deposition) tools, and it is still unknown whether the deposition temperature plays a role in LeTID formation. In this contribution, we subject sister wafers to different low temperature annealing steps (T_{var}< 500°C) in N_2 atmosphere *before* firing, after which we deposit the same Al_2O_3 layer on all samples.

Lifetime spectroscopy data also gave first hints on possible candidates responsible for the degradation due to the measured ratio of capture cross sections of the underlying lifetime limiting defects [11, 12]. Latest findings (*e.g.* [12-15]) indicate a direct involvement of hydrogen in the LeTID mechanism. Additionally to the annealing step in N_2 atmosphere, we also apply a H-plasma atmosphere during the annealing step to investigate the influence of hydrogen to the degradation and regeneration causing defect.

2 EXPERIMENTAL

To investigate the influence of a low temperature step before firing on LeTID and regeneration behavior, high quality B-doped p-type mc-Si sister wafers with comparable grain and defect structure from the middle of the ingot were processed to lifetime samples (5 x 5 cm^2). To further investigate the influence of sample thickness, half of the wafers were etched to a thickness of 150 µm, the rest to 170 µm. A scheme of the applied process sequence is given in Fig. 1. Half of the wafers were gettered via $POCl_3$ diffusion (55 Ω/□), after which the emitter was removed. Next, all samples were deposited with thin PECVD SiO_x at room temperature to protect the samples from contamination during low temperature annealing. The samples were annealed for different times (0.5-2 h) in a tube furnace at different temperatures (T_{var} <500°C).

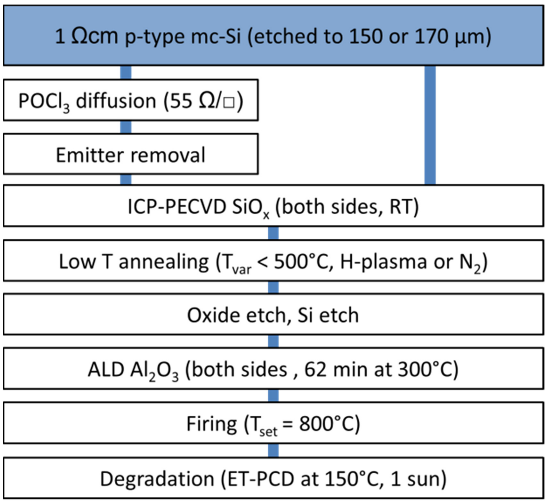

Figure 1: Process sequence of the investigated lifetime samples.

To investigate the influence of hydrogen on LeTID and regeneration behavior, half of the wafers were annealed in H-plasma atmosphere, which was realized by microwave-induced remote hydrogen plasma (MIRHP). The rest of the wafers were annealed in N_2 atmosphere. After SiO_x and silicon etching steps, all samples were deposited with double-sided 30 nm atomic layer deposition (ALD) Al_2O_3 at 300°C for a total of 62 min. Samples were fired in a belt furnace at a set temperature of 800°C.

For degradation, lifetime samples are held at a temperature of approx. 150°C under illumination with halogen lamps (1.0 ±0.1 suns). Effective minority charge carrier lifetime τ_{eff} is measured repetitively via photoconductance decay (PCD) at elevated temperature (ET) of 150°C. The lifetime is extracted at fixed excess charge carrier concentration of $\Delta n = 1.5 \times 10^{15}\ \mathrm{cm}^{-3}$. Additionally, spatially resolved lifetime maps were measured at certain stages of degradation and regeneration (after firing, at degraded state, after full regeneration) with the self-calibrated TR-PLI method [16] at room temperature (RT).

3 RESULTS

In the following either gettered or ungettered sample sets are shown and discussed. Nevertheless, all the observed results match qualitatively in each case.

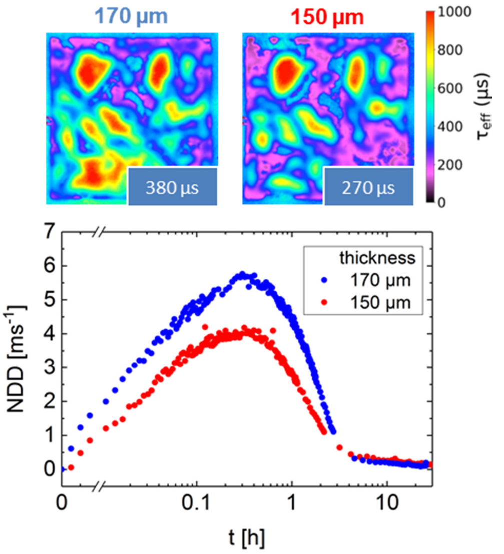

Figure 2: TR-PLI lifetime maps with harmonic average τ_{eff} values before degradation of two ungettered sister samples with thickness of 150 µm and 170 µm, respectively, annealed in N_2 atmosphere at 400°C for 30 min (top). Normalized defect density (NDD) of these two samples (150°C, 1 sun) calculated with extracted ET-PCD lifetimes (bottom).

3.1 Influence of sample thickness

TR-PLI lifetime maps of two ungettered sister wafers with thickness of 150 µm and 170 µm, respectively, are shown in Fig. 2. Also shown in Fig. 2 is the time-dependent normalized defect density, which is calculated using

$$\mathrm{NDD}(t) = \frac{1}{\tau_{\mathrm{eff}}(t)} - \frac{1}{\tau_{\mathrm{eff}}(0)} \tag{1}$$

where $\tau_{\mathrm{eff}}(t)$ and $\tau_{\mathrm{eff}}(0)$ is the extracted effective lifetime measured with ET-PCD at any given time and initial state, respectively. Both samples received a low temperature annealing step at 400°C in N_2 atmosphere before ALD Al_2O_3 passivation and firing. The thicker sample (170 µm) shows initial harmonic average τ_{eff} of 380 µs, the thinner sample (150 µm) only 270 µs.

Regarding NDD, both samples show pronounced LeTID and a following regeneration phase. While the thicker sample shows a stronger degradation, a complete regeneration to the starting value can be seen after a few hours in both samples. These observations are less pronounced but match qualitatively with [6], where also an influence of sample thickness on LeTID and regeneration was observed. In the model discussed in [6] a movement of impurities towards the wafer surface is assumed to be responsible for regeneration, and also a direct impact of wafer thickness on LeTID was detected.

3.2 Low-temperature annealing before firing

To investigate the influence of a low temperature annealing before firing, TR-PLI lifetime images of six gettered sister samples before degradation are shown in Fig. 3. Except the reference sample without additional annealing step before firing, they all received a low temperature annealing. Thereby, the temperature was held at 200°C, 300°C and 400°C for 30 min. Additionally at 300°C, the annealing time was increased to one or two hours.

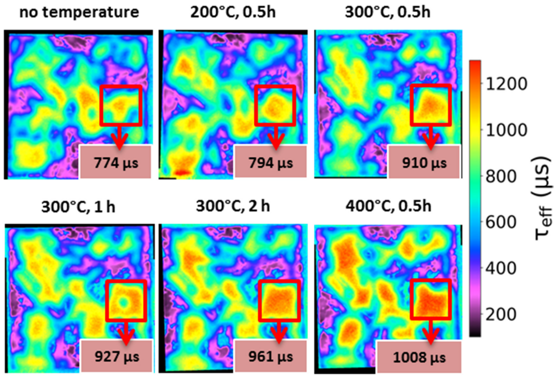

Figure 3: TR-PLI lifetime maps of gettered sister samples subjected to different low temperature annealing steps in N_2 atmosphere carried out before firing in the non-degraded state. The red squares highlight the change of one sample area with temperature and annealing time. The harmonic average τ_{eff} values of this area are outlined in the lower right corner.

It can be seen that a low temperature annealing step before firing improves initial τ_{eff}. As highlighted by red squares in Fig. 3, adding a low temperature step of 200°C improves the lifetime from 774 µs to 794 µs. Elevating the temperature further, the lifetime within the highlighted area increases up to 1008 µs with an annealing step at 400°C. When extending the low temperature annealing at 300°C from 30 min to 2 h, τ_{eff} increases again from 910 µs to 961 µs. This lifetime increase due to a low temperature step before firing might be caused by low temperature gettering of impurities internally or towards the surface layer.

The normalized defect density of the discussed samples is shown in Fig. 4. Within approx. 10 min of illumination, all the low temperature annealed samples have reached full degradation, but significantly different defect densities. The sample without additional low temperature annealing step does not show very strong LeTID, and degrades the least – comparable with the sample which underwent an annealing step at 300°C for 30 min. Interestingly, when increasing the time up to 1 h at 300°C, the sample shows the strongest degradation compared to the other investigated samples. Furthermore, all samples show stronger degradation when extending the low temperature annealing from 30 min to 1 h.

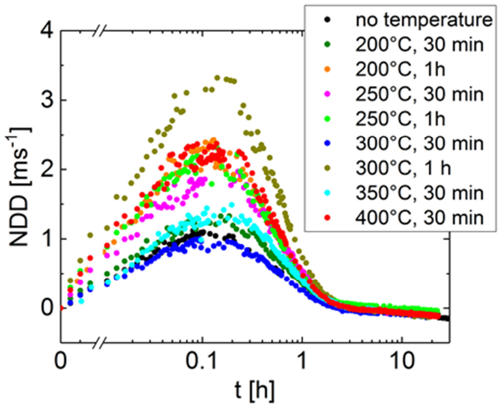

Figure 4: Normalized defect density of gettered sister samples with different temperatures and times during the low temperature annealing step in N_2 atmosphere carried out before firing.

While there is no obvious relation between temperature and LeTID kinetics visible, the low temperature annealing before surface passivation and firing changes the maximum LeTID defect density reached in the degradation/regeneration cycle. This means that the LeTID precursor/s is/are very sensitive to even small temperature variations below 500°C, and the effects of this temperature load is not erased by the following firing step.

3.3 Influence of hydrogen

TR-PLI lifetime maps directly after firing and after full degradation of two ungettered sister wafers which underwent an annealing step at 300°C for 30 min are shown in Fig. 5. Thereby the left sample was held in N_2 atmosphere while remote hydrogen plasma was present during the annealing of the sample shown on the right. Comparing the lifetime maps at initial state, it is obvious that the presence of H-plasma before ALD AlO_x passivation reduces τ_{eff}. The harmonic average τ_{eff} is decreased from 377 µs to 357 µs and regarding the spatially resolved maps, it can be seen that areas with high τ_{eff} are decreasing whereas areas with low τ_{eff} are increasing in τ_{eff}. This reduction in areas with high τ_{eff} is a first indication of the detrimental effect of hydrogen, which was already discussed in [15] and could lead to an issue regarding high performance mc-Si. The TR-PLI lifetime maps after full degradation give first hints that samples treated in H-plasma and therefore most probably containing more H in the Si bulk are more affected by LeTID, which was also recently observed in [17]. To further quantify these observations, the lifetime maps after firing and after full degradation were aligned to each other and NDD of each pixel was calculated according to Eq. 1. The resulting NDD maps are shown in the bottom row of Fig. 5. It can be seen that the sample with H-plasma present during annealing suffer much more from LeTID than the sample annealed in N_2 atmosphere.

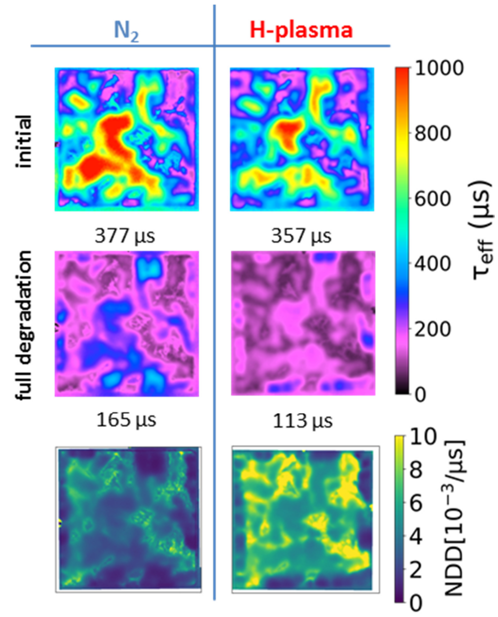

Figure 5: TR-PLI lifetime maps at initial state and after full degradation of two ungettered sister samples. Both samples underwent an annealing step at 300°C for 30 min but in different atmospheres (left column: N_2, right column: H-plasma). The last row shows the NDD maps, calculated according to Eq. 1 with the respective lifetime maps above.

Furthermore, a comparison of the NDD map with the initial TR-PLI lifetime map shows that areas with low initial τ_{eff} are more affected, but this is the case in both investigated samples. To further confirm these observations, time dependent NDD was calculated with ET-PCD data and is shown in Fig. 6.

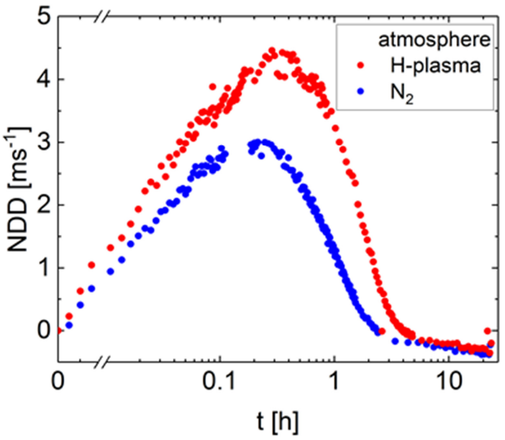

Figure 6: Normalized defect density calculated with ET-PCD data of the two sister samples displayed in Fig. 5.

A comparison of the differently treated samples shows clearly the detrimental impact of hydrogen on LeTID. The maximum NDD is significantly higher for the sample treated in H-plasma atmosphere. Additionally, a time shift of several minutes in reaching maximum NDD is visible. Interestingly, both samples regenerate completely. While for the sample annealed in N_2 atmosphere this is case after approx. 2 h, the sample treated in H-plasma atmosphere reaches the initial lifetime after 3 h. This might be due to the time shift in reaching maximum NDD.

It has to be said that the observed effect is more or less pronounced in the other investigated samples. But either the spatially resolved NDD maps or the NDD plots calculated with ET-PCD data always show the detrimental effect of hydrogen on LeTID. A possible explanation for the different strength of this effect might be that there is a strong dependency on the local defect structure or that the effect is very sensitive to small experimental variations (*e.g.*, temperature ramps during unloading of samples after low temperature annealing). Note that PCD data only show weighted average values of part of the sample and the extracted data can be misinterpreted. So when trying to evaluate measurements of mc-Si samples, a combination of spatially resolved measurements (*cf.* Fig. 5) and PCD measurements (*cf.* Fig. 6) is necessary and seems to be a good solution.

4 SUMMARY AND DISCUSSION

The influence of sample thickness, low temperature annealing *before* firing and the effect of a H-plasma on LeTID and regeneration could be shown on mc.Si wafers using data from TR-PLI and ET-PCD. Spatially resolved τ_{eff} and injection dependent τ_{eff} have been measured and delivered detailed results that allowed assertions on the different influences of the investigated parameters. The effect of sample thickness on LeTID and regeneration which was already discussed in [6] could be confirmed, and furthermore its influence on initial τ_{eff} could be demonstrated with spatially resolved lifetime maps.

A comparison of samples which underwent a low temperature anneal at different temperatures and annealing times *before* firing showed that lifetime measured directly after firing increases due to the low temperature step which might be caused by low temperature gettering internally or towards the surface layer. Regarding LeTID and regeneration, no obvious relation between annealing temperature and LeTID kinetics could be observed. Nevertheless, the chosen annealing temperatures clearly influence the visible maximum defect density, which indicates that LeTID precursor/s is/are very sensitive to even small temperature variations below 500°C of temperature steps carried out *before* firing, and the effects of these steps are not erased by the following firing step. These results help explain why the surface passivation deposition step itself affects LeTID, and ultimately why LeTID varies so much in mc Si-PERC solar cells from different manufacturers.

Furthermore, we could show the detrimental and positive effects of hydrogen introduced before ALD AlO_x surface passivation and firing on initial τ_{eff}. TR-PLI and ET-PCD measurements enabled a detailed comparison regarding LeTID and regeneration behavior of samples either annealed in N_2 or in H-plasma atmosphere. While hydrogen strengthens LeTID, all samples regenerate to their initial τ_{eff} value after a few hours.

5 ACKNOWLEDGEMENTS

Part of this work was supported by the German BMWi under contracts 0324204B, 0325763B and 0324001. The content of the publication is the responsibility of the authors. The authors would like to thank L. Mahlstaedt, B. Rettenmaier and J. Engelhardt for technical support.

6 REFERENCES

[1] K. Ramspeck, S. Zimmermann, H. Nagel, A. Metz, Y. Gassenbauer, B. Birkmann, A. Seidl, Proc. 27th EUPVSEC, Frankfurt/Main, Germany, 2012, 861.
[2] F. Fertig, K. Krauss, S. Rein, Physica Status Solidi RRL 9(1) (2014) 41.
[3] F. Kersten, P. Engelhart, H.-C. Ploigt, A. Stekolnikov, T. Lindner, F. Stenzel, M. Bartzsch, A. Szpeth, K. Petter, J. Heitmann, J. Müller, Solar Energy Materials and Solar Cells 142 (2015) 83.
[4] A. Zuschlag, D. Skorka, G. Hahn, Progress in Photovoltaics: Research and Applications 25(7) (2017) 545.
[5] A. Zuschlag, D. Skorka, G. Hahn, Proc. 43rd IEEE PVSC, Portland 2016, 1051.
[6] D. Bredemeier, D.C. Walter, J. Schmidt, Solar RRL 2 (2018) 1700159.
[7] J. Fritz, A. Zuschlag, D. Skorka, G. Hahn, Energy Procedia 124 (2017) 718.
[8] C.E. Chan, T.H. Fung, M.D. Abbott, D. Payne, A. Wellham, B. Hallam, R. Chen, S. Wenham, Solar RRL 1 (2017) 1600028.
[9] C.E. Chan, D.R. Payne, B.J. Hallam, M.D. Abbott, T.H. Fung, A.M. Wenham, B.S. Tjahjono, S.R. Wenham, IEEE Journal of Photovoltaics 6 (2016) 1473.
[10] F. Kersten, J. Heitmann, J.W. Müller, Energy Procedia 92 (2016) 828.
[11] A.E. Morishige, M.A. Jensen, D.B. Needleman, K. Nakayashiki, J. Hofstetter, T.-T.A. Li, T. Buonassisi, IEEE Journal of Photovoltaics 6(6) (2016) 1466.
[12] K. Nakayashiki, J. Hofstetter, A. Morishige, T. Li, D. Needleman, M. Jensen, T. Buonassisi, IEEE Journal of Photovoltaics 6(4) (2016) 860.
[13] T.H. Fung, M. Kim, D. Chen, C.E. Chan, B.J. Hallam, R. Chen, D.N.R. Payne, A. Ciesla, S.R. Wenham, M.D. Abbott, Sol. En. Mat. Sol. Cells 184 (2018) 48.
[14] D. Bredemeier, D.C. Walter, J. Schmidt, AIP Conference Proceedings 1999 (2018) 130001.
[15] D. Chen, P.G. Hamer, M. Kim, T.H. Fung, G. Bourret-Sicotte, S. Liu, C.E. Chan, A. Ciesla, R. Chen, M.D. Abbott, B.J. Hallam, S.R. Wenham, Solar Energy Materials and Solar Cells 185 (2018) 174.
[16] D. Kiliani, G. Micard, B. Steuer, B. Raabe, A. Herguth, G. Hahn, Journal of Applied Physics 110 (2011) 054508.
[17] M.A. Jensen, A. Zuschlag, D. Skorka, S. Wieghold, A.E. Morishige, G. Hahn, T. Buonassisi, Journal of Applied Physics 124(8) (2018) 085701.